The physical properties of oxygen-deficient perovskite $SrPbO_{3-\delta}$

2006 J. Phys.: Condens. Matter 18 8551

(http://iopscience.iop.org/0953-8984/18/37/013)

INSTITUTE OF PHYSICS PUBLISHING JOURNAL OF PHYSICS: CONDENSED MATTER

J. Phys.: Condens. Matter **18** (2006) 8551–8561 doi:10.1088/0953-8984/18/37/013

The physical properties of oxygen-deficient perovskite $SrPbO_{3-\delta}$

B Hadjarab[1], A Bouguelia[2], M Kadi-Hanifi[1] and M Trari[2,3]

[1] Laboratoire des Solutions Solides, Faculty of Physics, (USTHB) BP 32 16111, Algiers, Algeria
[2] Laboratoire de Stockage et de Valorisation des Energies Renouvelables, Faculty of Chemistry, (USTHB) BP 32 16111, Algiers, Algeria

E-mail: hbkrim@yahoo.fr and mtrari@caramail.com

Received 9 April 2006, in final form 20 July 2006
Published 1 September 2006
Online at stacks.iop.org/JPhysCM/18/8551

Abstract

The transport properties of oxygen-deficient perovskite $SrPbO_{3-\delta}$ with mixed lead valency were investigated down to 4.2 K. The small δ-value (0.059), determined from iodometry, is due to the inert lone pair Pb^{2+} that does not enjoy regular octahedral coordination in spite of collective electron behaviour. The oxide exhibits a temperature-independent magnetic susceptibility consistent with itinerant electrons. The sign of carriers like polarons is that of n-type conductivity coming from the balance charge via oxygen extraction. The thermal variation of conductivity and thermopower reveal the existence of an energy gap. The conduction mechanism occurs by polaron hopping in conformity with small activation energy. The metal–insulating transition seems to be of Anderson type, resulting from the disorder of oxygen vacancies. At low temperature, the conductivity was fitted to a variable range hopping $\ln(1/\rho) \propto T^{-4}$. A comparison with $SrSnO_3$ will be reported. The covalency of Sn–O raises the antibonding conduction state of 5s parentage and increases the forbidden gap from 1.78 to 3.30 eV.

1. Introduction

Since the discovery of superconductivity in the system $BaPbO_3$–$BaBiO_3$ with a transition temperature of 13.5 K [1], a great deal of attention has been paid to advanced researches with this system both from the scientific and the applied point of view [2, 3]. However, the main open question, related to intrinsic limitations with the perovskite oxides, which remains unclear is the absence of superconductivity in spite of the existence of mixed valence states over homologous compounds. One may expect to find superconductivity with this class of materials; it has been found in the spinel $LiTi_2O_4$ with an average one-half Ti 3d electron [4].

[3] Author to whom any correspondence should be addressed.

$BaBiO_3$ has been the research topic within the framework among non-copper superconducting oxides. In terms of simple band structure, the oxide with one unpaired electron ($6s^1$) per formula unit would be expected to be metallic. However, it displays an insulating behaviour and involves a charge ordering of Bi^{III} and Bi^{IV} where the ions occupy two sets of non-equivalent octahedra [5]. Larger and smaller BiO_6 octahedra alternate with a tendency of the charge in Bi–O bonds to disproportionate to form a charge density wave. No ESR signal has been found and the small temperature-independent susceptibility agrees with a degenerate semiconductivity. The oxidation states were apparently Bi^{3+} and Bi^{5+} with paired electrons which are known to exist in oxides but not Bi^{4+}.

In this perspective, a special attention was focused on valency states in deficient $SrBO_{3-\delta}$ with the stereochemically inactive lone pair for heavy B-metals, where B denotes an element of IV_A group of periodic table. The existence of mixed valencies $N/(N-2)$ permits the altering of physical properties. $SrBO_3$ can easily lose oxygen, a well known phenomenon in the perovskite and rutile oxides chemistry, and this would imply an n-type conductivity via a charge balance. Moreover, $SrBO_3$ is known to be among the main candidates for chemical sensors, detectors of moisture and electrodes for solar light batteries [6].

$SrPbO_3$ belongs to the family of intergrowth $AO(ABO_3)_n$ providing a sequential evolution of magnetic and transport properties. It is known that reduced dimensionality lowers the critical temperature in superconductors but in our case superconductivity has not been observed down to 4.2 K. Dark brown $SrPbO_3$ has been characterized by a wide variety of techniques, and has been a subject of controversy, and there is still an ambiguity in the determination of transport properties. Dotz *et al* [7] have found a p-type semiconductivity with an increase of F_O centres due probably to the known volatility of lead. The oxide exhibits a small range of oxygen deficiency and is classified as a narrow band gap semiconductor (SC) because of its two-dimensional half-filled conduction band (CB). $SrPbO_3$ was prepared as previously described; the transport properties are modified by the introduction of oxygen vacancies and the electrons are believed to move in a narrow CB of Pb: 6s/O: 2p character with an effective mass close to the free electron mass. It has been reported to have an orthorhombic symmetry with possible space group *Pnmn* [8]. This enables a comparison of the physical properties with $SrSnO_3$ already available in our laboratory.

While $SrPbO_3$ exhibits a n-type conductivity as synthesized, $SrSnO_3$ can be made n-type by heating under moderate reducing atmospheres (vacuum or metal getter) or by doping with a non-isovalent cation on the electronically active Sr or B sublattices [9]. The conduction follows an Arrhenius-type law which changes to the variable range hopping (VRH) at low temperatures. The larger covalency of the Pb–O bond increases the Pb 6s–O 2p overlap and consequently raises the antibonding σ^* band with the formation of a gap unlike that of $BaPbO_3$. However, the perovskite structure is isotropic and the large tilt of PbO_6 octahedra around the main axis weakens the chemical bond and lowers the σ^* band with respect to the cubic perovskite $SrSnO_3$, resulting in a smaller gap.

2. Experimental details

High-purity $SrPbO_3$ was prepared by solid state reaction from stoichiometric amounts of PbO_2 and dried $SrCO_3$, both of purity >99.5%. The mixture was homogenized in an agate mortar and calcined in air at 850 °C with an isothermal step of 6 h at 600 °C to preclude loss of PbO_2 by volatilization. Then the sample was reground, pelleted under 2 kbar and finally sintered at 940 °C. For comparative purposes, $SrSnO_3$ was synthesized from prefired SnO_2 and $SrCO_3$ at 1200 °C followed by air-quenching; this served as the starting material for further heat treatment to prepare $SrSnO_{3-\delta}$. The reduction was achieved by heating sintered pellets at

Table 1. The experimental physical properties of perovskites $SrBO_3$.

Oxide	Colour	Symmetry	d_{exp} (g cm^{-3})	Lattice constants (nm)	Z	t	$n \times 10^{20}$ (cm^{-3})	$\rho^{-1}_{300\,K}$ (Ω^{-1} m^{-1})	ΔE (meV)	E_g (eV)	T_M (K)
$SrPbO_3$	Dark brown	Orthorhombic SG: $Pbnm$	7.44	$a = 0.5851(6)$ $b = 0.5968(9)$ $c = 0.8324(4)$	4	0.92	15.52	0.4	5	1.82	∼55
$SrSnO_3$	White	Cubic SG: $Pm\bar{3}m$	6.09	$a = 0.4042(8)$	1	0.96	2.88	3×10^{-3}	51	3.25	∼140

1000 °C in an evacuated silica tube. The reduction does not occur as easily as in TiO_2 and the process was considerably speeded up under dynamic vacuum (<1 mbar); we were unsuccessful in obtaining large oxygen deficiency.

The powder x-ray diffraction (XRD) was performed using a Phillips diffractometer with a Cu target anode. The data were obtained by using an increment of 0.5° and a counting time of 40 s over an angular interval of 10°–80°. The cell parameters were refined from the analysis of the XRD profile using the least square method and Si as internal standard. The density d_{exp} was determined by the hydrostatic method in toluene because of its wetting properties. The elemental composition was established by inductively coupled plasma: the Sr/Pb ratio was equal to unity within the experimental errors. Total lead was determined by titration with EDTA, and iodometric titration was used to evaluate the average oxidation state of lead. ∼20 mg of powder was dissolved in concentrated HCl with KI excess under inert atmosphere, and the liberated I_2 was back titrated by $Na_2S_2O_3$ (10^{-2} M) according to the global reaction ($Pb^{4+} + 2S_2O_3^{2-} \rightarrow Pb^{2+} + S_4O_6^{2-}$).

The IR spectra were obtained by using a Perkin Elmer spectrometer. The reflectance diffuse spectra were recorded on a Carry 500 spectrophotometer in the range 300–2000 nm with MgO-coated integrating-sphere reflectance attachment. The dc conductivity ($1/\rho$) was measured by the four-probe collinear method on sintered pellets whereas the temperature dependence of thermopower S ($=\Delta V/\Delta T$) in a home-made equipment, and the induced emf was measured by a differential electrometer with an input impedance of 10^{12} Ω. The precision was dependant on the quality of thermal contact and the samples were held between sinks to ensure good electrical and thermal contact. The small heat conductivity made it possible to use a large temperature gradient and to continue the measurement down to liquid helium temperature.

3. Results and discussion

Because of the isothermal step at 600 °C, less than 1% in the weight loss of lead was observed by EDTA titration. A fast heating results in loss of PbO_2 as evidenced from the appearance of Sr_2SnO_4 lines in the XRD spectrum. The patterns of $SrPbO_3$ and $SrSnO_3$, depicted in figure 1, were single phases and refined respectively in the space groups *Pbnm* and *Inbm*. The lattice constants are gathered in table 1 along with the main physical properties. The densities d_{exp} were determined to be about 95% of theoretical bulk values.

From a crystallochemical point of view, $SrPbO_3$ cannot adopt an ideal perovskite structure. The passage from Pb- to Sn-compound induces a contraction of the lattice constants and a decrease of tolerance factor t (considering Shannon ionic radii) raising the symmetry respectively from orthorhombic to cubic. This implies a decrease in the unit cell volume V/Z

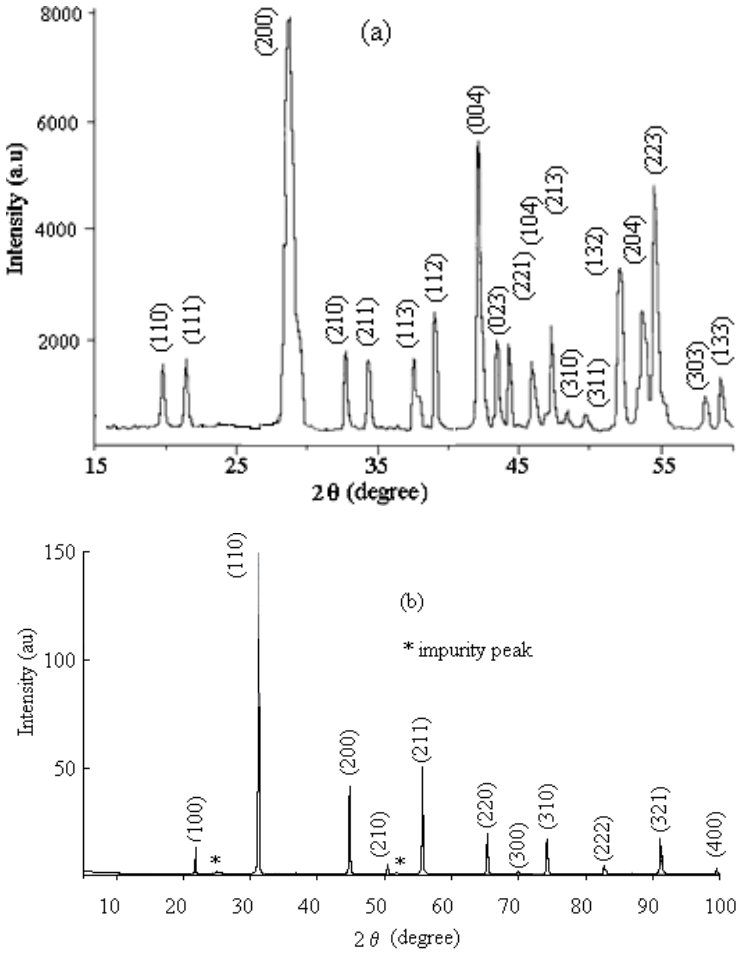

Figure 1. X-ray diffraction patterns of $SrPbO_3$ (a) and $SrSnO_3$ (b).

from 0.0726 to 0.0661 nm^3 through the substitution, a behaviour ascribed to the smaller ionic radius of Sn^{4+} (0.069 nm) with respect to Pb^{4+} (0.0775 nm) in six-fold coordination [10] for the same nuclear charge, Z being the number of formula weights per unit cell (table 1). The type of cooling process (slowly or quick frozen) does not affect the final structure of $SrPbO_3$ but makes the oxygen deficiency variable[4]. Keester *et al* [11] have previously reported the dielectric properties of $SrPbO_3$ with a phase transition but no anomaly was observed by differential scanning calorimetry in our case. The cell parameters remain somewhat constant despite the oxygen removal, a behaviour ascribed to the generation of divalent lead upon reduction $\{r(Pb^{2+}) = 0.119$ nm$\}$. Pb^{2+} has too large a size to enter the octahedral site and possesses an inert $6s^2$ lone pair of electrons which has the effect of producing irregular coordination polyhedra. It has been suggested that a partial substitution of Sr^{2+} by Pb^{2+} seems probable in the crystal structure [7]. However, the oxide displays a SC behaviour and our opinion is that the fact that the lattice constants do not change significantly with respect to the pure compound

[4] In contrast, the structure of $SrSnO_3$ depends on the type of cooling. When furnace cooled it crystallises in an orthorhombic symmetry. When quenched, it changes to a cubic unit cell.

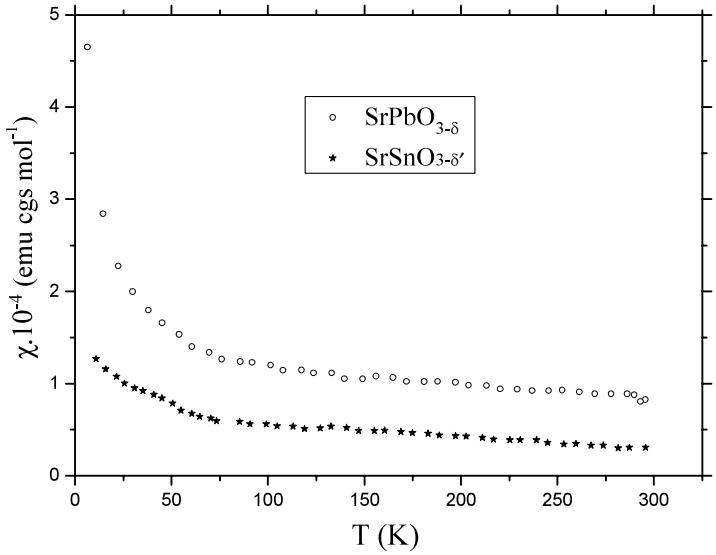

Figure 2. Magnetic susceptibility versus absolute temperature for $SrPbO_{3-\delta}$ and $SrSnO_{3-\delta'}$.

(when treated under O_2 flow and cooled slowly) indicates that the stereochemical inert pair $6s^2$ is delocalized in the CB. In addition, the peak of the electrochemical $Pb^{2+/4+}$ couple is missing in the intensity–potential curve (in KOH media) because of the electron delocalization of the lone pair (manuscript in preparation).

The ideal ABO_3 perovskite structure consists of a three-dimensional array of BO_6 octahedra sharing corners with 180° B–O–B angles. The tilting of PbO_6 octahedra around the crystallographic *c*-axis forms the zigzag chains doubling the lattice parameters.

The structure enables a comparison of physical properties of both perovskites. An evaluation of the paramagnetism contribution of itinerant electrons for $SrPbO_3$, assuming a parabolic band, is given by [12]

$$\chi = \left(\frac{4m^*\mu_B^2}{h^2 3^{1/3}}\right) n^{2/3} \left(1 - \frac{m^2}{3m^{*2}}\right)$$

where m is the electron rest mass, m^* the effective mass and n the electron concentration. χ is nearly temperature independent in the range 20–300 K (figure 2). Below 20 K there is a sharp upturn which might be due to localized electron paramagnetic centres. χ_{spin} is of same order of magnitude as the contribution of ion diamagnetism and agrees with the existence of collective electrons. However, it is difficult to extract the part of the susceptibility due to the itinerant electrons; the low susceptibilities imply a delocalization of ns^2 electrons. A value of m^* of ∼1.5 m for $SrPbO_3$ is deduced, enhanced by electron–electron correlation as expected for small density doping and polaron hopping.

The concentration n in a solid could be increased by alloying and a discontinuous transition from insulating to metallic state would occur; as applied to a doped SC it should be observed when $n^{1/3}a_H = 0.25$ [13]; the Bohr radius a_H of a shallow donor is a_H (nm) $= 0.053\varepsilon \cdot m/m^*$, ε being the dielectric constant. As already mentioned, $SrBO_3$ has no appreciable range of non-stoichiometry and does not form grossly oxygen-deficient phases in contrast to titanates where $SrTiO_{2.5}$ has been reported [14]. It is well known that the tendency to produce definite oxides is all the greater when the difference of electron negativities between ions is high. In addition, lessening the unit-cell size lowers the mobility of oxygen ions and in this

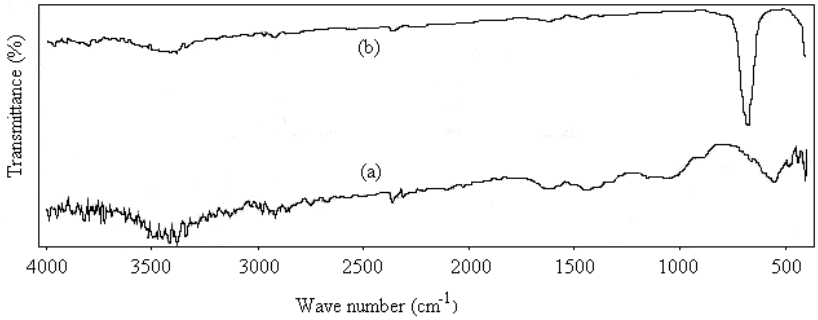

Figure 3. IR spectra of $SrPbO_3$ (a) and $SrSnO_3$ (b).

way the degree of reduction from $SrPbO_3$ to $SrSnO_3$.[5] The mean oxidation state of lead, determined by iodometric titration, was found to be 3.88, which corresponds to δ- and n-values respectively of 0.059 and 1.55×10^{21} cm^{-3}. The low δ-value lies in the crystal chemistry of lead and tin: both ions B^{4+} have nd^{10} closed shell electronic configuration and $SrBO_3$ are expected to be insulators. The next lower ion B^{2+} has too large a size to enable octahedral coordination. However, the fact that XRD and chemical analysis showed no appreciable change in composition particularly with the tin compound and the fact that the oxides exhibit a moderate conductivity would mean that the stereochemical ns^2 pair is delocalized in the CB of cationic B-ns parentage.

In perovskites, the conductivity has the same origin in deficient and doped specimens. The electron configuration should be perturbed by the substitution of foreign atoms having different electronic structure. In the solid solution $Sr_{1-x}La_xSnO_3$ studied previously[6], lanthanum enters $SrSnO_3$ as La^{3+} (d^{10}) onto Sr-sites. The charge neutrality requires the generation of two electrons ($5s^2$: Sn^{2+}). Consequently, the n-value for $SrSnO_{3-\delta'}$ can be evaluated by interpolation from a calibration plot of ρ versus La^{3+} composition through the relation $\rho = (ne\mu_e)^{-1}$ on the assumption that each substituted lanthanum yields one electron per unit formula [15], e being the electron charge. n is in fact twice the concentration of Sn^{2+} and was deduced from d_{exp} (6.09 g cm^{-3}). A value of 2.88×10^{20} cm^{-3} was found which corresponds formally to a δ'-value of 9×10^{-3}.

The IR absorption bands of inorganic oxides in the range 100–1500 cm^{-1} are ascribed to optically active vibrations. We may try to interpret the spectra in the light of the obtained data and those reported in the literature [16, 17]. Figure 3 shows that the IR spectra are essentially featureless from 1000 up to 4000 cm^{-1}. There is one vibrational stretching associated with B–O bonds in $SrBO_3$ whose frequencies increase from 564 to 672 cm^{-1} respectively for the Pb- and Sn-compound, leading to an increase of the length of the B–O bond and consequently to a weaker bond for $SrPbO_3$. The absorption peak located at 1630 cm^{-1}, more pronounced for lead oxide, probably appeared due to water adsorption while handling the sample in air.

Preliminary work has been done to evaluate the optical gap E_g for $SrBO_3$. In figure 4 are represented the reflectance diffuse spectra of both oxides. $SrPbO_3$ exhibits an absorption in the visible region extending down to 1500 nm and the broad shoulder accounts for the dark brown colour. The data do not provide a clear-cut absorption edge which is expected for indirect transitions. Instead, a continuous gradual increase in optical absorption at decreasing

[5] For $SrSnO_{3-\delta'}$ dissolved in $HClO_4$ under inert atmosphere, the value of Sn^{2+} concentration, determined by polarography, was below the detection of the apparatus but sufficient to induce an insulator–metal transition.

[6] The solution exists only for $x \leqslant 0.02$, above which the stable pyrochlore $La_2Sn_2O_7$ appears.

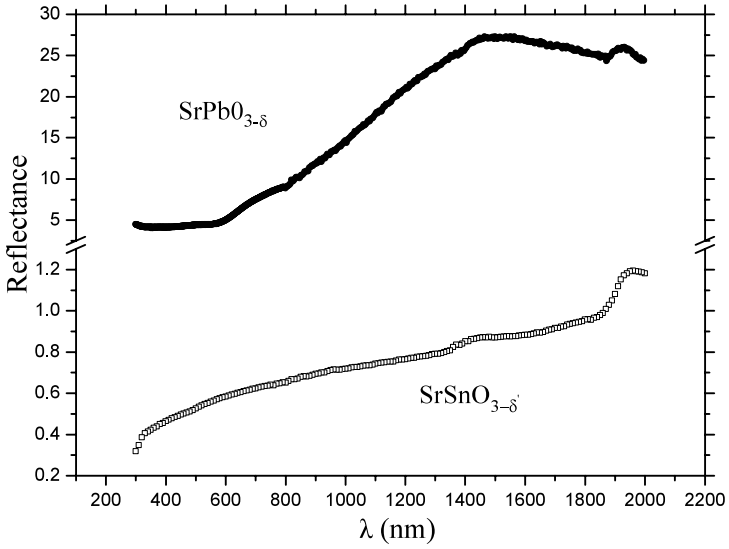

Figure 4. Diffuse reflection spectra of $SrPbO_{3-\delta}$ and $SrSnO_{3-\delta'}$.

wavelength is observed. The energy E_g was estimated using the wavelength at the absorption edge from the intersection of the straight line through the steep portion of the edge with the nearly horizontal line; a value of ∼1.82 eV was deduced. The detailed studies yielded an optical transition at 1.78 eV and will be reported in a future paper. In contrast, pure $SrSnO_3$ is transparent in the visible region and up to ∼300 nm. Upon reduction the material becomes a SC and a broad absorption appears which increases towards the visible region. The calculations give a direct transition at 3.25 eV. The oxygen vacancies and defect states at energy levels within the band gap are responsible for the optical transitions (band tailing). The CB may be considered as resulting from a mixture of B: ns/O: 2p orbitals. In spite of the smaller difference of electron negativities between lead and oxygen which would theoretically strengthen the chemical bond, a bending of Pb–O–Pb entities with an angle of 146° accounts for a small overlap and the weaker covalency. The tilt of the PbO_6 octahedra around the main axis of the ideal perovskite, equal to 22°, would be responsible for the lower optical gap. In contrast, $SrSnO_3$ crystallizes in a cubic structure with an angle Sn–O-Sn equal exactly to 180° that leads to a less stable antibonding CB resulting in a larger gap E_g.

The basic physical parameters which govern the insulator–metal transition have been reported early by Mott [18] and a deficiency on the O-site may result in a polaron SC to localization of distant vacancies. Thermoelectric data combined to electrical conductivity allow an understanding of the conduction mechanism. Since the resistivity measurements were performed on polycrystalline sintered discs, it is not possible to account accurately for the intergrain resistance effect.

As is known, the electrical properties in perovskites are strongly correlated to oxygen deficiency, and the discussion of transport properties is based on thermoactivated hopping between mixed valencies. The n-type conductivity is ascribed to oxygen vacancies via a charge compensation mechanism to the controlled valency form, wherein lead atoms undergo a valency change $Pb^{IV} \rightarrow Pb^{II}$. To our knowledge, the Pb^{III} ion has never been reported in the literature. In Pb_2O_3, Pb^{II} ions are located between layers of distorted $Pb^{IV}O_6$ octahedra whereas Pb_3O_4 consists on chains of octahedra sharing opposite edges and linked to each other

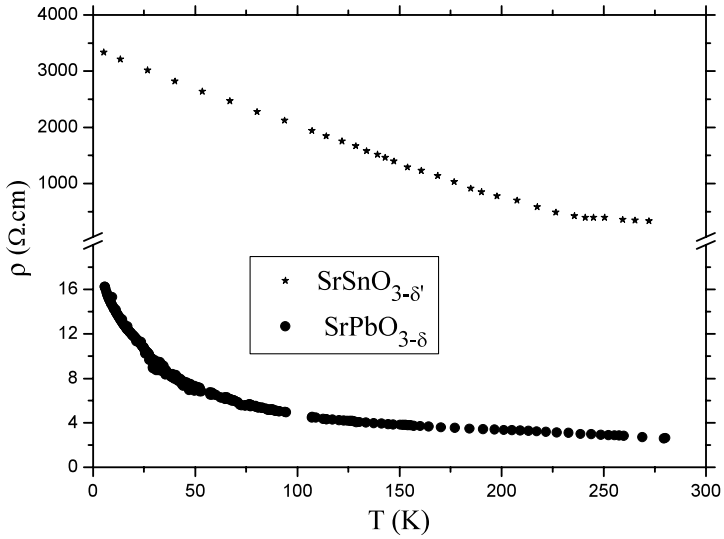

Figure 5. Electrical resistivity versus absolute temperature for $SrPbO_{3-\delta}$ and $SrSnO_{3-\delta'}$.

by divalent Pb^{II}. In our case, lead is accommodated in a mixed valent state in equivalent sites as required by the charge neutrality and $SrPbO_{3-\delta}$ belongs to class II in the Day and Robin classification [19]. The ions Pb^{2+} and Pb^{4+} are distributed in octahedral sites sharing corners, and electrons can migrate easily between $Pb^{2+/4+}$. Hence $SrPbO_{3-\delta}$ is expected to be a good conductor with a small activation energies ΔE. The compound is at the edge of the insulator–metal transition and the band tails are more pronounced to localization through the mobility edge. The same remark holds for $SrSnO_{3-\delta'}$.

For a metal, the resistivity ρ tends towards a finite value when T approaches zero. The thermal variation of ρ illustrates a semiconducting behaviour ($d\rho/dT < 0$) for both materials (figure 5) and is contrasted to that reported previously by Lobanov *et al* [20]. The authors reported a SC–metal transition at ∼130 K with increasing temperature and which does not occur in our case. In a SC in which the charge carriers obey the Maxwell–Boltzmann statistic, i.e. $kT \gg E_f$, the resistivity decreases with T^{-1}. Above a temperature T_M (table 1), the plots of $\log(1/\rho)$ versus $1000/T$ (not shown here) were fitted by a least square method to straight lines with ΔE-values given in table 1. The change in the slope of $\log \rho^{-1}$ versus T^{-1} is due to thermal lattice vibrations which affect the electron scattering when T increases and the temperature-independent resistivity can be ascribed to electron scattering by oxygen vacancies. Below ∼60 K, a logarithm plot of the mobility μ versus T for $SrPbO_3$ was found to be linear but with a slope of approximately 0.5 excluding the lattice scattering mechanism, i.e. the mobility is not limited by oxygen vacancies. Data for fully oxidized $SrSnO_3$ are not presented as this oxide is found to be insulating with $\rho_{300\ K} > 10^6\ \Omega$ cm and this rules out extrinsic conduction over the investigated temperature range.

The order of magnitude of ρ and S suggest that the mechanism conduction occurs predominantly by polaron hopping in conformity with low ΔE-values. The differences with others [21] may be ascribed to various oxygen content when the oxide is cooled under different conditions.

Mott pointed out that the insulator–metal transition occurs when the mean free path extends over many interatomic distances. For a fixed electron concentration, the mobility edge approaches the Fermi level when $k_F\, l$ is low (the Ioffe–Regel criterion), the latter characterize

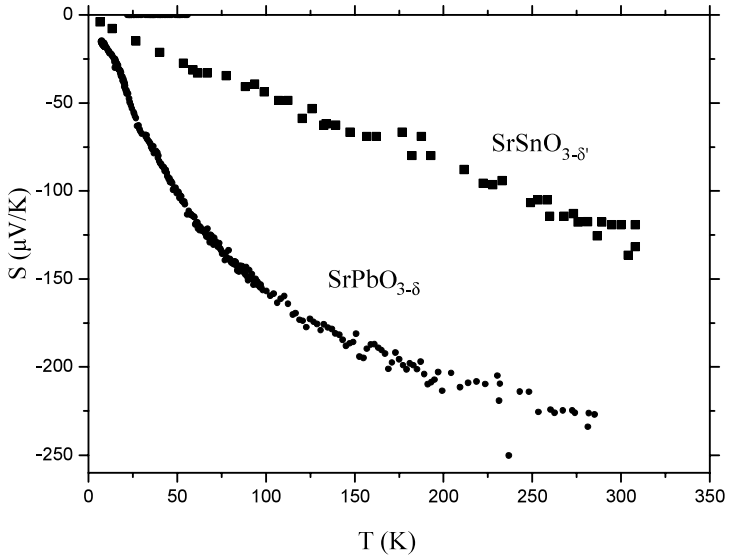

Figure 6. Temperature variation of thermopower S of $SrPbO_{3-\delta}$ and $SrSnO_{3-\delta'}$.

the extent of disorder in the material. For the transition to conduction between delocalized states in the vicinity of the mobility edge, S is given by [18]

$$S = \left(\frac{\pi^2 k^2 T}{3e}\right)\left(\frac{\mathrm{d}\ln\rho^{-1}}{\mathrm{d}E}\right)_{Ef};$$

the relation is valid for systems in which the concentration n does not change significantly. Indeed, the linear increase of $|S|$ (figure 6) indicates an electron mobility μ that is thermally activated and a constant number of carriers. In both cases, the conduction mechanism should be dominated by electrons as S remains negative and much larger for $SrSnO_3$, indicating a lower carrier density (table 1). In addition, for $SrPbO_3$ the ΔE value (5 meV) is so small that all donors are ionized for $T > 60$ K, above which the concentration n reaches its maximal value. Consequently, the decrease of ρ with T comes only from the thermal enhancement of the mobility μ $(= 1/\rho ne)$.

The oxygen deficiency of $SrPbO_{3-\delta}$ would predict a concentration n (table 1), so that for every extracted oxygen, two conductive electrons are generated. For such a concentration, the average separation l between vacancies is found to be ∼0.9 nm assuming a random distribution, a value very close to that calculated (∼1 nm) from the formula

$$l_{\mathrm{theo}} = \left(\frac{3kTm^*\mu^2}{e^2}\right)^{1/2},$$

e being the electron charge. The observed resistivity $\rho_{300\ \mathrm{K}}$ was ∼2.5 Ω cm, in poor agreement with that calculated (0.012 Ω cm) from the relation $1/\rho_{\mathrm{min}} = 0.05\ e^2 2\pi (h\ l)^{-1}$ [13]. For $SrSnO_3$, l/l_{theo} was found to be ∼3 and $1/\rho_{\mathrm{min}} \sim 0.021$ Ω cm.

The absence of linear dependence of $\ln 1/\rho$ versus T^{-1} at low temperature results from VRH. The existence of a polaron contribution in $SrBO_3$ leads to a phonon-assisted conductivity for $T > \theta_{\mathrm{D}}/4$ giving rise to a mass enhancement, θ_{D} being the Debye temperature. Indeed, S does not follow exactly the expected tendency because of the electron–phonon interaction which leads to an increase of the effective mass m^* which generally appears below 50 K. The strong evidence for phonon-assisted VRH in the present system, corroborated by the Anderson

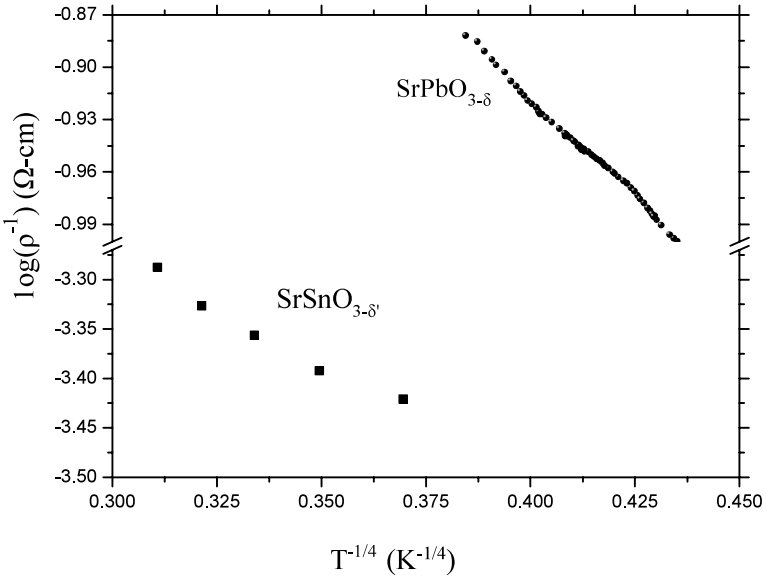

Figure 7. Plot of $\log(\rho^{-1})$ versus $T^{-1/4}$ for $SrPbO_{3-\delta}$ and $SrSnO_{3-\delta'}$.

localization, is based on the hazardous potential due to oxygen vacancies distributed randomly in the crystal lattice. Mott [18] showed that the hopping to nearest sites, which follows the Arrhenius-type law, transforms below T_M to VRH according to $\ln \rho^{-1} \propto T^{-4}$ (figure 7).

As mentioned above, the replacement of Pb by Sn leads to a stronger ionicity of the Sr–O bond and strengthens the σ-bonding of Sn^{4+}: 5s–O^{2-}: 2p character. The constancy in energy of the σ-valence band in $SrMO_3$ regardless of the nature of B, coupled with a destabilization of σ^*-bonding, results in a wide gap E_g for $SrSnO_3$. Moreover, the smaller covalency of the Pb–O bond would have the effect of narrowing the conduction band of Pb: 6s/O: 2p parentage and affects the density of states at the energy level E_f, a result supported by thermopower measurements where the absolute value increases from Pb to Sn. In this perspective, photoelectrochemical studies of $SrPbO_3$ are continuing in an effort to elucidate the energy diagram and will be reported in a subsequent paper.

4. Conclusion

$SrBO_{3-\delta}$ was synthesized by solid reaction and the transport properties were investigated down to liquid helium temperature. Both oxides crystallize in the perovskite structure and it was instructive to compare their physical properties. They exhibit a small temperature-independent and positive susceptibility, consistent with itinerant electron behaviour and an effective mass approaching the rest mass electron for $SrPbO_3$. Lead and tin are accommodated in mixed valent states $B^{2+/4+}$ through oxygen extraction as required by the electroneutrality condition. The conduction occurs by polaron hopping with small activation energies. The thermopower showed that charge carriers are of n-type and the linear temperature dependence indicates an electron mobility thermally activated rather than the doping density as being responsible. At low temperatures, the conductivity follows a variable range hopping where $\ln \rho^{-1}$ is proportional to $T^{-1/4}$. The larger covalency of the Sn–O bond raises the antibonding σ^* energy; this would have the effect of widening the conduction band of Sn 6s/O 2p character and to increase the optical gap of $SrSnO_3$.

Acknowledgments

The authors thank the Faculty of Chemistry (Algiers) for supporting this research. They are greatly indebted to Mr T Gaceb for his technical assistance.

References

[1] Sleight A W, Gillson J L and Bierstedt P E 1975 *Solid State Commun.* **17** 27
[2] Fu W T, Martens H C F and Maaskant W J A 1997 *Solid State Commun.* **101** 149
[3] Martens H C F, Fu W T, Reedijk J A, Adriaanse L J and Broom H B 1998 *Physica* C **297** 149
[4] Diebold U 2003 *Surf. Sci. Rep.* **48** 53
[5] Cox D E and Sleight A W 1976 *Solid State Commun.* **19** 969
[6] Bajpai P K, Ratre K, Pastor M and Sinha T P 2003 *Bull. Mater. Sci.* **26** 461
[7] Droz V A, Ekino T, Gabovich A M, Pekala M, Ribeiro R A, Shevchenko A D and Uvarov V M 2005 *J. Phys.: Condens. Matter* **17** 7407
[8] Shannon R D 1971 *J. Solid. State. Chem.* **3** 184
[9] Parkash O M, Mandal K D, Christopher C C, Sastry M S and Kumar D 1994 *Bull. Mater. Sci.* **17** 253
[10] Shannon R D 1976 *Acta Crystallogr.* A **32** 751
[11] Keester K L and White W B 1970 *J. Solid State Chem.* **68** 2
[12] Wilson A H 1953 *The Theory of Metals* 2nd edn (Cambridge: Cambridge University Press)
[13] Mott N F and Davis E A 1979 *Electronic Processes in Non-Crystalline Materials* (Oxford: Clarendon)
[14] Gong W, Yun H, Ning Y B, Datars W R, Greedan J E and Stager C V 1991 *J. Solid. State. Chem.* **90** 320
[15] Trari M 1994 *PhD Thesis* Bordeaux
[16] Nyquist R A and Kagel R D 1971 *Infrared Spectra of Inorganic Compounds* vol. 128 (New York: Academic) p 108
[17] Azad A M, Hashim M, Baptist S, Badri A and Haq A Ul 2000 *J. Mater. Sci.* **35** 5475
[18] Mott N F 1974 *Metal–Insular Transition* (London: Taylor and Francis)
[19] Day P and Robin R 1966 *Adv. Inorg. Chem.* **10** 247
[20] Lobanov M V, Kopnin E M, Xenikos D, Grippa A Ju, Antipov E V, Capponi J J, Marezio M, Julien J P and Tholence J L 1997 *Mater. Res. Bull.* **32** 983
[21] Droz V A, Gabovich A M, Pekala M, Boychuk V N, Moiseev D P and Nedilko S A 2002 *J. Alloys Compounds* **346** 17